An efficiency analysis of an induction motor with direct torque and flux control at a hot rolling mill.

Induction motor efficiency analysis: direct torque, flux control

by Dr. Rupert Gouws, North-West University

In this study, two scenarios were evaluated: where the induction motor was controlled at a constant speed with a variable thickness slab, and where the speed of the induction motor was controlled according to the thickness of the slab.

Both scenarios used the speed as reference to control the torque and flux of the induction motor. A comparison on the energy consumption of the induction motor for both scenarios was done by means of a detailed simulation model. The simulation model for this specific case study is explained in detail. The results obtained showed an increase in the efficiency of the induction motor from the original system (scenario 1) to the improved system (scenario 2).

This article presents the efficiency analysis of an induction motor with direct torque and flux control at a hot rolling mill in South Africa.

A hot rolling mill plant near Witbank, Mpumalanga, was investigated as a case study. The hot rolling mill plant has an installed capacity to produce 4000 Mt of steel bars in a month.

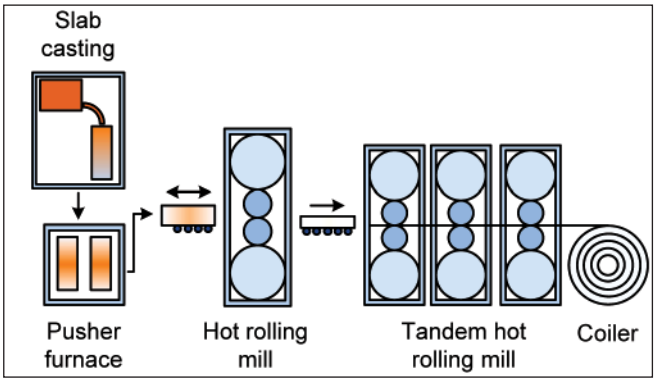

Fig. 2: Hot strip/rolling production process.

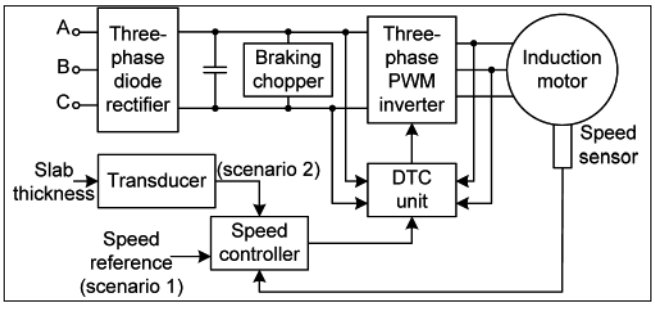

Fig. 3: Overview of the control process.

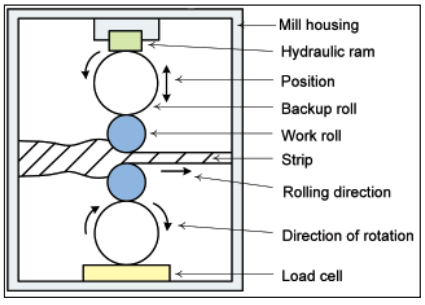

Fig. 1: Four-high hot rolling mill stand.

The monthly average production is currently 3400 Mt (85% of the installed capacity).

The diameter of the bars produced vary from 8 mm to 20 mm. The demand of the plant is 1000 kVA and the daily energy consumption is 10 MWh. The parameters and specifications of the hot rolling mill plant were used in the design process of the simulation model.

Hot rolling mills

Rolling occurs when metal is passed through a pair of rolls. Hot rolling occurs when the temperature of the metal is above the recrystallisation temperature, while cold rolling occurs when the temperature of the metal is below the recrystallisation temperature.

Fig. 1 provides a diagram of a four-high hot rolling mill stand. This rolling

Parameter	Dimension
Distance between stands	3900 mm
Work roll diameter	505 mm
Backup roll diameter	1265 mm
Roll face	1870 mm
Rolling force	30 000 kN
Strip width	1235 mm
Overall reduction	80%
Asynchronous motor	110 kW

Table 1: Hot strip/rolling mill plant parameters.

mill is also known as a reduction mill. A slab is passed through two work rollers which reduce the thickness of the slab. The reduction in thickness is caused by high compression applied by hydraulic rams. The reduction in strip thickness causes a temperature rise at the roll gap, which is cooled by air and a lubricant solution.

Hot rolling mills are usually equipped with sensors to measure the roll force at each stand, strip tension force, strip thickness, work roll speed, roll gap actuator (hydraulic ram) position and strip speed. The backup rolls are installed to provide rigid support to the working rolls and to prevent bending under rolling load.

Fig. 2 provides an overview diagram of the hot strip/rolling production process. After the refining and alloying (slab casting) processes, the molten metal is cast into semi-continuous casters of 10 to 25 t slabs.

The slabs are then pre-heated in the pusher furnace and hot rolled by a single-stand hot rolling mill. The slabs are then passed through a tandem hot rolling mill which provides strips with a thickness of between 2,5 and 6 mm. The strips can then be coiled at a temperature of approximately 300°C.

Simulation case study

This section provides the design of the simulation model from the specifications and parameters of the hot rolling mill plant.

Table 1 provides the parameters of the hot rolling mill. These were used in the design process of the simulation model for this specific case study.

Fig. 3 provides an overview of the control process for this specific case study. From this figure it can be seen that a three-phase diode rectifier supplies a braking chopper. This is a dynamic braking chopper with a DC bus capacitor which absorbs the energy produced when the

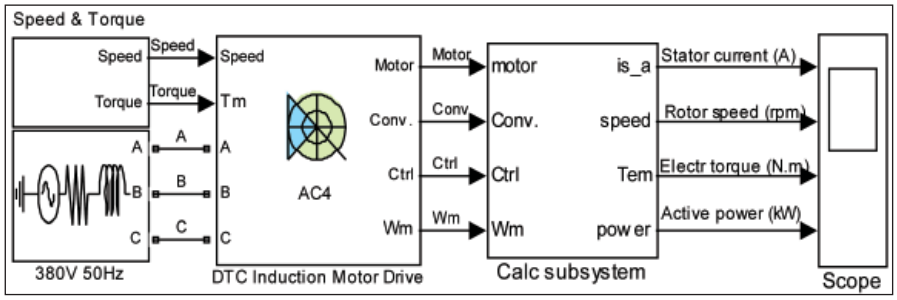

Fig. 4: Overview of the simulation model.

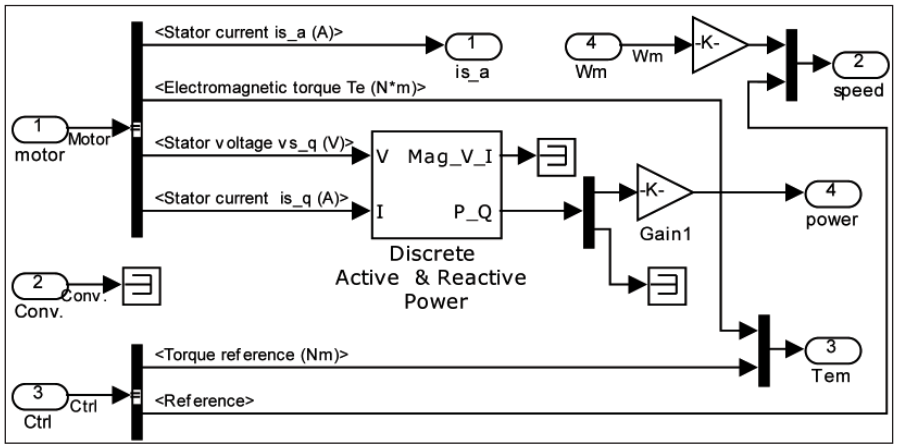

Fig. 5: Calc subsystem.

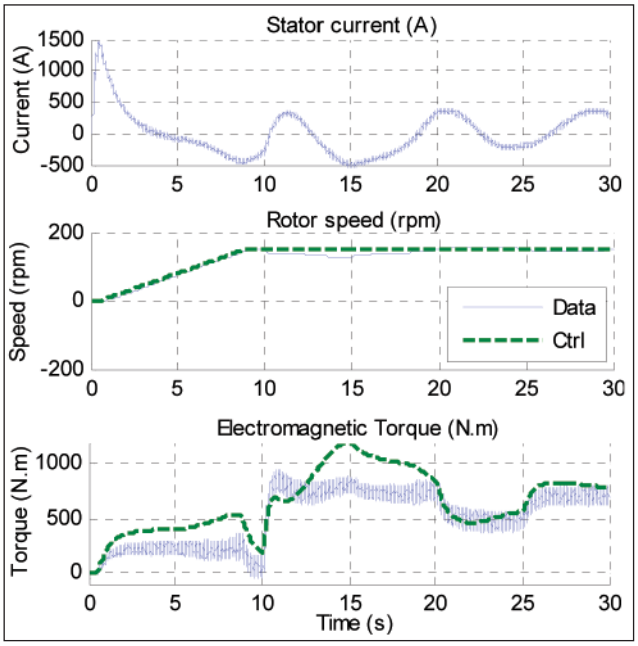

Fig. 6: Scenario 1 – model analysis.

motor decelerates. The output of the braking chopper is connected to a three-phase PWM voltage source inverter which supplies the induction motor. A speed controller uses the speed of the induction motor (measured by means of a speed sensor). The speed controller uses a PI controller to produce flux and torque references for the DTC unit. The thickness of the slab is measured by means of a position sensor. A transducer converts this signal to a reference speed.

The torque and flux are calculated in the DTC unit and compared to their respective references. An optimal switching table is then used to generate the inverter switching pulses.

For scenario 1, the speed reference is kept constant and a variable thickness slab is selected. For scenario 2, the speed is controlled according to the thickness of the slab.

For the simulation model design

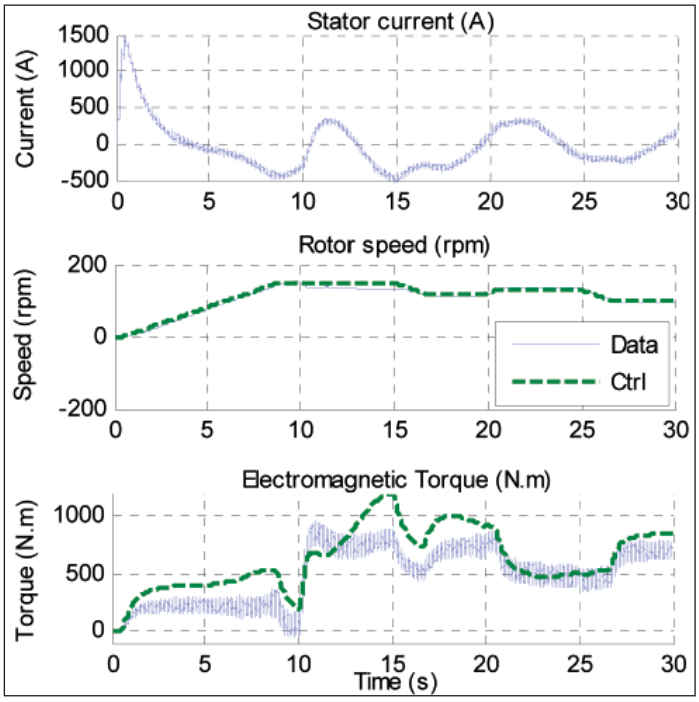

Fig. 7: Scenario 2 – model analysis.

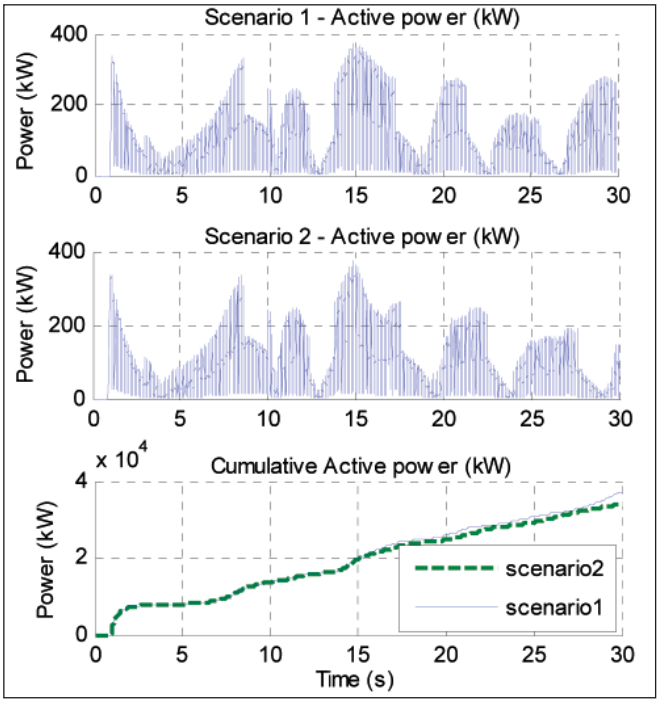

Fig. 8: Combined power results.

(see Fig. 4) an AC4 block from the SimPowerSystems library was used. The block models the direct torque control (DTC) induction motor drive with the braking chopper for the motor. A 110 kW induction motor (see Table 1 for the plant parameters) was used for this simulation.

The three-phase diode rectifier, braking chopper, three-phase PWM inverter, DTC unit and speed controller are simulated by means of the AC4 block which was adapted to incorporate the dynamics and parameters of this specific case study.

The speed and torque characteristics for the two scenarios are simulated by means of the speed and torque subsystem.

Fig. 5 provides the calc subsystem which performs the calculations for the stator current, speed, electromagnetic torque and power.

Results

The results are divided into scenario 1 (speed kept constant with variable slab thickness), scenario 2 (speed controlled according to slab thickness) and combined results (comparison between the results of scenarios 1 and 2).

Scenario 1

In this scenario the speed is constantly controlled at 150 rpm and a variable slab thickness is selected. In this scenario the rotor is given 10 s to start up before a slab is processed. Fig. 6 shows the stator current, rotor speed and electromagnetic torque for this scenario.

The stator current peaks around 1500 A during start-up. The rotor speed dips the moment the slab enters the process. The actual speed (data) then follows the control speed (Ctrl) closely. The actual electromagnetic torque (data) follows the control torque (Ctrl) closely.

Scenario 2

In this scenario the speed is controlled according to the thickness of the slab. The same variable slab thickness is selected for both scenarios. In this scenario the rotor is again given 10 s to start up before a slab is processed. Fig. 7 shows the stator current, rotor speed and electromagnetic torque for scenario 2.

The stator current again peaks around 1500 A during start-up and the rotor speed dips the moment the slab enters the process, but the speed is now controlled according to the thickness of the slab. The actual speed (data) closely follows the control speed (Ctrl). The actual electromagnetic torque (data) closely follows the control torque (Ctrl).

Combined results

In this section the active power for the two scenarios is evaluated. Fig. 8 shows the active power and cumulative active power for scenarios 1 and 2. A lot of spikes are visible on the active power signals. This is caused by the switching of the three-phase PMW voltage source inverter.

The result of the first 10 s for both scenarios is the same, since this is the start-up time of the rotor. Thereafter, different profiles can be seen. From the cumulative active power graph it can be seen that the cumulative power after 30 s for scenario 2 is less than that of scenario 1. The cumulative energy consumption resulted to an average improvement of 4,44% from scenario 1 to scenario 2.

Conclusion

A simulation model was designed in Matlab Simulink to obtain results and evaluate the two scenarios. The specifications and parameters of the physical system were used in the design process of the simulation model.

It can be seen from the combined results of the two scenarios that the cumulative power for scenario 1 is higher than that of scenario 2. The cumulative energy consumption resulted in an average improvement of 4,44% from scenario 1 to scenario 2.

Acknowledgment

This paper was presented at the 2011 ICUE conference and is published here with permission.

Contact Dr. Rupert Gouws,
North-West University,
Tel 018 299-4900,
rupert.gouws@nwu.ac.za